Propagation of Sound through a Real Jet Flowfield

C. H. Liu* and L. Maestrello†
NASA Langley Research Center, Hampton, Va.

The sound propagation of harmonic disturbances through a real jet flowfield which contains mean flow gradients in pressure and velocities, has been studied. A finite-difference approximation for the equations which govern the acoustic disturbance is obtained for a subsonic axisymmetric jet in terms of acoustic pressure and acoustic energy flux. Experimental results are used to describe the mean flowfield of a model jet. The equations are solved numerically using a Newton-type iterative scheme. The directivity at various distances from a point source located at two jet diameters downstream of the jet exit on its centerline compared qualitatively well with the numerical result of Schubert[7] and with the experimental result of Grande.[15] The computations are made for acoustic energy density flux crossing an ideal plane at the smallest possible distance from the jet, in the area where the homogeneous wave equation is reasonably well satisfied. This result also compared qualitatively well with the experiment of Maestrello.[1]

Introduction

THIS work is an extension of a program at NASA Langley Research Center concerning the investigation of noise generated by a jet, and follows the work by Maestrello[1] in which the acoustic energy density flux on a plane near the jet boundary and its relationship to the far field sound was obtained. This information is relevant only to the sound arising from sources inside the jet as it emanates from the outer jet boundary. The problem still exists to define the sources of sound within the jet and to understand how sound is propagated outward through the jet into the far field.

The distribution of the radiation due to these sources depends on the resultant strength of the superposition of a number of multipole fields.[2] The sources embedded in the moving jet are distributed in space time, more or less randomly, and the resultant disturbance interacts with the local flowfield stimulating the fluid motion so that acoustic energy is extracted from, as well as imparted to, the flow. This mechanism tends to indicate that conditions inside the jet depend on nonlinear interactions among mean and fluctuating quantities. The manner in which this mechanism can be handled is not yet in sight, and therefore we do not consider this aspect further. Regardless, however, of the detailed source mechanism, the problem of the propagation of acoustic disturbances from such sources can be formulated and investigated. Progress has been made toward understanding how harmonic disturbances propagate through the jet stream. Examples for an idealized jet flowfield are the work of Lilley,[3] Mungur et al.,[4] Plumblee,[5] Graham,[6] Schubert,[7] and Mani.[8] Using a linearized convective wave equation, Pao[9] has obtained closed-form far-field solutions for sound emission from moving quadrupole sources in a parallel shear layer.

The intent of the present work is to significantly aid in the identification of the mechanism of sound propagation arising from true sources inside the stream by studying the propagation of harmonic disturbances through a realistic jet which contains mean flow gradients in pressure and velocities. The modeling of the sound field results in two coupled complex elliptic partial differential equations for the amplitude and phase of the pressure which are solved by a finite-difference technique using a Newton-type iterative procedure. This approach will provide only a partial answer to the problem, because the source may not be adequately describable by harmonic solution inside the jet; in addition, since the physical properties of the flow vary from point to point, one is required to have a knowledge of the random variation of the flow as the sound wave passes through it. Both of these aspects are being investigated as part of the follow-up program of the propagation of sound through a real jet flowfield.

Although this work is concerned with jet flow, the approach used is applicable to other problems of sound propagation for which a mean flowfield can be given, such as acoustic atmospheric propagation, flow over a surface, and so forth.

Formulation of the Problem

Convective Wave Equation

The problem at hand is to derive the convective wave equation for the pressure and to study the propagation of sound through the flowfield of an axisymmetric spreading jet. An acoustic source is placed within the potential core of a static jet. The origin of the coordinate system is fixed at the source, Fig. 1, while the coordinate of the flowfield is fixed at the virtual origin of the jet.

The governing equations in spherical coordinates (r, θ, ϕ) for an ideal fluid are:

the equation of continuity

$$d\rho/dt + \rho\nabla \times \vec{\mathbf{U}} = 0 \tag{1}$$

Euler's equation

$$\begin{aligned}\rho\left[\frac{d\mathbf{U}}{dt} - \frac{\mathbf{V}^2+\mathbf{W}^2}{r}\right] &= -\frac{\partial \mathbf{P}}{\partial r}\\ \rho\left[\frac{d\mathbf{V}}{dt} + \frac{\mathbf{UV}}{r} - \frac{\mathbf{W}^2\cot\theta}{r}\right] &= -\frac{1}{r}\frac{\partial \mathbf{P}}{\partial \theta}\\ \rho\left[\frac{d\mathbf{W}}{dt} + \frac{\mathbf{W}}{r}(\mathbf{U}+\mathbf{V}\cot\theta)\right] &= -\frac{1}{r\sin\theta}\frac{\partial \mathbf{P}}{\partial \phi}\end{aligned} \tag{2}$$

and energy equation

$$d\mathbf{P}/dt - \gamma\mathbf{P}/\rho\, d\rho/dt = 0 \tag{3}$$

where $\mathbf{P}$ is the pressure, ρ the density, $\gamma = C_p/C_v$ the constant ratio of specific heats, and the Eulerian derivative

$$d/dt \equiv \partial/\partial t + \vec{U} \times \nabla = \partial/\partial t + U(\partial/\partial r) + (\mathbf{V}/r)(\partial/\partial\theta) + (\mathbf{W}/r\sin\theta)(\partial/\partial\phi)\cdot \vec{\mathbf{U}} \equiv (\mathbf{U},\mathbf{V},\mathbf{W})$$

is the velocity vector. $\mathbf{U}$, $\mathbf{V}$, $\mathbf{W}$ are the velocity components in the r, θ, ϕ directions, respectively.

Presented as Paper 74-5 at the AIAA 12th Aerospace Sciences Meeting, Washington D.C., January 30–February 1, 1974; submitted March 4, 1974; revision received July 15, 1974.

Index categories: Aircraft Noise, Aerodynamics (Including Sonic Boom); Subsonic and Transonic Flow.

* NAS-NRC Resident Research Associate. Associate Member AIAA.

† Head, Aeroacoustics Section, Noise Control Branch. Member AIAA.

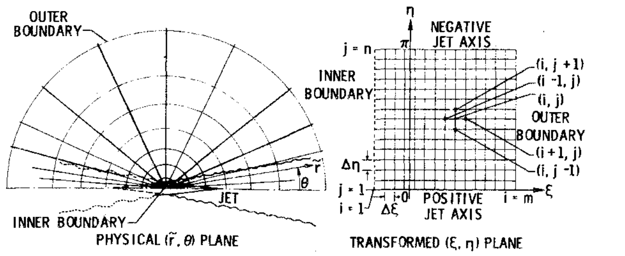

Fig. 1 Coordinate transformation.

For the perturbation of flow quantities, one can write the flow variables $\vec{\mathbf{U}}$, $\mathbf{P}$, and $\boldsymbol{\rho}$ in the form

$$\vec{\mathbf{U}} = \vec{U}+\vec{u}, \quad \mathbf{P} = P_o+p, \quad \boldsymbol{\rho} = \rho_o+\rho \tag{4}$$

where $\vec{U}$, P_o, and ρ_o are the steady-state mean velocity, pressure, and density, respectively, and $\vec{u}$, p, and ρ are their corresponding variations due to the sound wave, such that

$$\left|\frac{\vec{u}}{\vec{U}}\right| \ll 1, \quad \left|\frac{p}{p_o}\right| \ll 1, \quad \text{and} \quad \left|\frac{\rho}{\rho_o}\right| \ll 1 \tag{5}$$

The local speed of sound is then given by

$$a^2 = \frac{\gamma \mathbf{P}}{\boldsymbol{\rho}} = \frac{\gamma P_o}{\rho_o}\left[1 + \left(\frac{p}{P_o} - \frac{\rho}{\rho_o}\right) + \text{higher order terms}\right]$$

On substituting Eqs. (4) and (5) into Eqs. (1–3), two sets of governing equations are obtained. Zeroth order equations which govern the steady-state mean flow ($\vec{U}$, P_o, ρ_o) are the same as that for ($\vec{\mathbf{U}}$, $\mathbf{P}$, $\boldsymbol{\rho}$), that is, Eqs. (1–3).

First-order equations which are linearized versions of Eqs. (1–3) and which are applicable to the propagation of sound waves if the conditions, Eq. (5), are satisfied are:

continuity

$$Ds/Dt+\nabla \cdot \vec{u}+\vec{u} \cdot \nabla(\ln \rho_o) = 0 \tag{6}$$

momentum

$$\gamma\left[\frac{Du}{Dt} + \vec{u} \cdot \nabla u - \frac{2}{r}(Vv+Ww)\right] = -a_o^2\left[\frac{\partial\sigma}{\partial r} + (\sigma-s)\frac{\partial \ln p_o}{\partial r}\right] \tag{7a}$$

$$\gamma\left[\frac{Dv}{Dt} + \vec{u} \cdot \nabla V + \frac{1}{r}(Uv+Vu-2Ww\cot\theta)\right] = -a_o^2\left[\frac{1}{r}\frac{\partial\sigma}{\partial\theta}(\sigma-s)\frac{1}{r}\frac{\partial \ln P_o}{\partial\theta}\right] \tag{7b}$$

$$\gamma\left[\frac{Dw}{Dt} + \vec{u} \cdot \nabla W + \frac{Wu+Uw}{r} + \frac{1}{r}(Vw+Wv)\cot\theta\right] = -a_o^2\left[\frac{1}{r\sin\theta}\frac{\partial\sigma}{\partial\phi} + (\sigma-s)\frac{1}{r\sin\theta}\frac{\partial \ln P_o}{\partial\phi}\right] \tag{7c}$$

energy

$$\frac{D\sigma}{Dt} + \vec{u} \cdot \nabla(\ln P_o)+\gamma(\nabla \cdot \vec{u}) = 0 \tag{8}$$

where $D/Dt = \partial/\partial t+\vec{U} \cdot \nabla$ is the commutative operation of time mean motion, $a_o^2 = \gamma P_o/\rho_o$, $\sigma = p/P_o$, and the condensation $s = \rho/\rho_o$.

To solve Eqs. (6–8) for the acoustic variables $\vec{u}$, σ, and s, one has to know the spatial variations of steady-state mean flow quantities $\vec{U}$, P_o, and ρ_o either by solving mean flow equations or by experimental measurements. In order to derive a wave equation for the acoustic pressure, one has to combine Eqs. (6–8). Taking the derivative, D/Dt, of Eq. (8) with the aid of mean flow equations, one obtains

$$\frac{D^2\sigma}{Dt^2} + \frac{D}{Dt}\left[\vec{u} \cdot \nabla \ln P_o\right] + \gamma\frac{D}{Dt}(\nabla \cdot \vec{u}) = 0 \tag{9}$$

In view of Eqs. (6) and (8), one finds that

$$D\sigma/Dt = \gamma(Ds/Dt) \tag{10}$$

By performing the operation

$$\frac{1}{r^2}\frac{\partial}{\partial r}[\text{Eq. (7a)}\, r^2] + \frac{1}{r\sin\theta}\frac{\partial}{\partial\theta}[\text{Eq. (7b)}\sin\theta] + \frac{1}{r\sin\theta}\frac{\partial}{\partial\phi}[\text{Eq. (7c)}]$$

and adding Eq. (9) there results a convective wave equation

$$\begin{aligned}
&\frac{D^2\sigma}{Dt^2} - a_o^2\nabla^2\sigma - [a_o^2\nabla^2(\ln P_o)+\nabla a_o^2 \cdot \nabla(\ln P_o)](\sigma-s) - \\
&\nabla a_o^2 \cdot \nabla\sigma - a_o^2[\nabla(\sigma-s) \cdot \nabla(\ln P_o)] = \\
&-\vec{u} \cdot \nabla\left[\frac{D}{Dt}(\ln P_o)\right] - \frac{D}{Dt}[\vec{u} \cdot \nabla \ln P_o] + \\
&\gamma\left\{\frac{\partial\vec{U}}{\partial r} \cdot \nabla u + \frac{1}{r}\frac{\partial\vec{U}}{\partial\theta} \cdot \nabla v + \frac{1}{r\sin\theta}\frac{\partial\vec{U}}{\partial\phi} \cdot \nabla w + \right. \\
&\frac{\partial\vec{u}}{\partial r} \cdot \nabla U + \frac{1}{r}\frac{\partial\vec{u}}{\partial\theta} \cdot \nabla V + \frac{1}{r\sin\theta}\frac{\partial\vec{u}}{\partial\phi} \cdot \nabla W + \\
&\frac{2U}{r}(\nabla \cdot \vec{u}) - \frac{2}{r}\left(\vec{U} \cdot \frac{\partial\vec{u}}{\partial r}\right) + \\
&\frac{2V}{r}\left[\cot\theta\left(\frac{1}{r\sin\theta}\frac{\partial w}{\partial\phi} + \frac{u}{r} + \frac{v\cot\theta}{r}\right)\right] + \\
&\frac{2W}{r}\left[-\frac{\cot\theta}{r}\frac{\partial w}{\partial\theta}\right] + \frac{2}{r}\left[\frac{u}{r}\frac{\partial V}{\partial\theta} - v\frac{\partial V}{\partial r}\right] + \\
&\left.\frac{2}{r}\left[-w\frac{\partial W}{\partial r} - w\frac{\cot\theta}{r}\frac{\partial W}{\partial\theta} + (u+v\cot\theta)\left(\frac{1}{r\sin\theta}\frac{\partial W}{\partial\phi}\right)\right]\right\}
\end{aligned} \tag{11}$$

where ∇^2 is the Laplacian in spherical coordinates. The left-hand side of the Eq. (11) contains all terms involving acoustic pressure, and the right-hand side contains all interaction terms between acoustic velocities and mean flow quantities and their derivatives. Far away from the jet flow, all the terms except the first two in Eq. (11) vanish, leaving the well-known homogeneous wave equation which, under isentropic conditions, governs linear acoustics in a uniform medium at rest. Equation (11) describes how sound, once generated, is propagated through a moving fluid with gradients in velocities and pressure. It should be noted that the scattering effect due to the presence of turbulence has been neglected.

Intermittency and Mean Flowfield

Results obtained in previous sections indicate that in order to evaluate the acoustic field through a nonuniform jet one has to acquire information on the mean flow variables and their gradients.

Measurements were made on a cold subsonic axisymmetric air jet exciting from a long pipe nozzle with a diameter of 0.0625 m and with mean exit velocity of $U_j = 213$ m/sec. Measurements of the mean and fluctuating velocity field were made with a constant temperature hot-wire anemometer using a pair of cross wire anemometer probes. The signals from the hot wire were linearized and adjusted to equalize the sensitivity of the U component of the mean velocity field of the two channels. The intermittency, mean velocity, and pressure field were reported previously in Ref. 10, where the mean values are expressed in a functional form for numerical computation (see Fig. 2). Figure 2 shows that the outer boundary of the jet is defined by a cone with vertex at the virtual origin of the jet, situated at 2.6 nozzle diameters upstream of the nozzle exit. The half-cone angle is 11° from the jet axis which corresponds to a spread of approximately 1% turbulence. The flow mixing at large downstream distances from the nozzle exit is more rapid than in the vicinity of the jet exit as indicated by the entrained flow angle which shows a 90° angle at large distances and diminishes with decreasing distance from the nozzle exit.

The flowfield being discussed is an axisymmetric spreading jet with no swirl; the mean velocities, pressure, and density fields

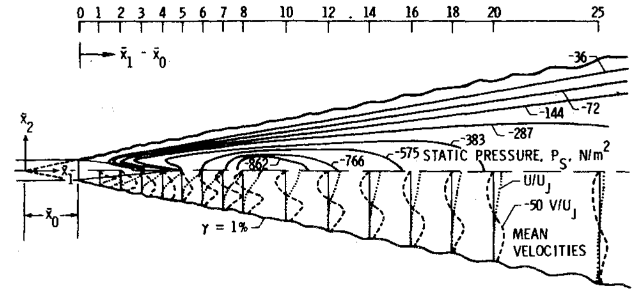

Fig. 2 Flowfield of the jet; $U_j = 213$ m/sec, $d_o = 0.0625$ m.

are functions of the radial distance r and the azimuthal angle θ. Thus, the mean flow is described by

$$\vec{U} = [U(r,\theta), V(r,\theta), 0], \quad P_o = P_o(r,\theta), \quad \rho_o = \rho_o(r,\theta) \tag{12}$$

Incorporating Eq. (12) into Eq. (11) results,

$$\frac{D^2\sigma}{Dt^2} - a_o^2\nabla^2\sigma - [a_o^2\nabla^2(\ln P_o) + \nabla a_o^2 \cdot \nabla(\ln P_o)](\sigma - s) - \nabla a_o^2 \cdot \nabla\sigma - a_o^2 \cdot [\nabla(\sigma - s) \cdot \nabla(\ln P_o)] = -\vec{u} \cdot \nabla\frac{D}{Dt}(\ln P_o) - \frac{D}{Dt}[\vec{u} \cdot \nabla \ln P_o] + \gamma\left\{\frac{\partial\vec{U}}{\partial r} \cdot \nabla u + \frac{1}{r}\frac{\partial\vec{U}}{\partial\theta} \cdot \nabla v + \frac{\partial\vec{u}}{\partial r} \cdot \nabla U + \frac{1}{r}\frac{\partial\vec{u}}{\partial\theta} \cdot \nabla V + \frac{2U}{r}(\nabla \cdot \vec{u}) - \frac{2}{r}\left(\vec{U} \cdot \frac{\partial\vec{u}}{\partial r}\right) + \frac{2V}{r}\left[\cot\theta\left(\frac{u}{r} + \frac{v\cot\theta}{r}\right)\right] + \frac{2}{r}\left(\frac{1}{r}\frac{\partial V}{\partial\theta}u - \frac{\partial V}{\partial r}v\right)\right\} \tag{13}$$

Equation Governing Pressure

The present analysis adopts the following solution for the normalized acoustic pressure σ

$$\sigma = [\tilde{\sigma}(\tilde{r},\theta)/\tilde{r}]\exp\{i[k(\tilde{r},\theta)\tilde{r} - \omega t]\} \tag{14}$$

where $\tilde{r} = r/d_o$. The expressions for the acoustic velocities u and v are similar.

Schubert[7] suggested that one possible way of reducing the large number of grid points required for the numerical solution of the pressure is to separate the phase and amplitude. By substituting Eq. (14) into the momentum equation (7), one can express the acoustic velocities in terms of normalized pressure σ. Using this relationship and its partial derivatives, the convective wave equation of the normalized pressure σ [Eq. (13)] is split into two nonlinear equations for the phase and amplitude by taking the real and the imaginary part of the equation.

$$\begin{aligned} &\text{Real part} && F = G_1H_1 + G_2H_2 - C = 0 \\ &\text{Imaginary part} && G = G_1H_2 + G_2H_1 - D = 0 \end{aligned} \tag{15}$$

where

$$G_1 = \lambda_o^2 + \frac{1}{\tilde{r}}\frac{\partial\tilde{a}^2}{\partial\tilde{r}} - \frac{\gamma-1}{\gamma}\left[\nabla^2\ln P_o - \frac{1}{\tilde{r}}\frac{\partial\ln P_o}{\partial\tilde{r}} + \nabla\tilde{a}^2 \cdot \nabla\ln P_o\right] + 2\lambda_o\vec{M}\cdot\nabla\beta - \nabla\tilde{a}^2\cdot\nabla\alpha - \frac{\gamma-1}{\gamma}\nabla\ln P_o \cdot \nabla\alpha - \tilde{a}^2\frac{\cot\theta}{\tilde{r}^2}\frac{\partial\alpha}{\partial\theta} + (M_1^2 - \tilde{a}^2)\left[\frac{\partial^2\alpha}{\partial\tilde{r}^2} + \left(\frac{\partial\alpha}{\partial\tilde{r}}\right)^2 - \left(\frac{\partial\beta}{\partial\tilde{r}}\right)^2\right] + (M_2^2 - \tilde{a}^2)\frac{1}{\tilde{r}^2}\left[\frac{\partial^2\alpha}{\partial\theta^2} + \left(\frac{\partial\alpha}{\partial\theta}\right)^2 - \left(\frac{\partial\beta}{\partial\theta}\right)^2\right] + (\vec{M} \cdot \nabla M_1) \cdot \left(\frac{\partial\alpha}{\partial\tilde{r}} + \frac{1}{\tilde{r}}\right) + (\vec{M} \cdot \nabla M_2)\frac{1}{\tilde{r}}\frac{\partial\alpha}{\partial\theta} + \frac{M_1M_2}{\tilde{r}}\left[2\left(\frac{\partial^2\alpha}{\partial\tilde{r}\partial\theta} - \frac{\partial\beta}{\partial\tilde{r}}\frac{\partial\beta}{\partial\theta}\right) + \left(2\frac{\partial\alpha}{\partial\tilde{r}} - \frac{1}{\tilde{r}}\right)\frac{\partial\alpha}{\partial\theta}\right]$$

$$G_2 = -2\lambda_o\vec{M} \cdot \nabla\alpha - \nabla\tilde{a}_o^2 \cdot \nabla\beta - \frac{\gamma-1}{\gamma}\tilde{a}^2\nabla\ln P_o \cdot \nabla\beta - \tilde{a}^2\frac{\cot\theta}{\tilde{r}^2}\frac{\partial\beta}{\partial\theta} + (M_1^2 - \tilde{a}^2)\left(\frac{\partial^2\beta}{\partial\tilde{r}^2} + 2\frac{\partial\alpha}{\partial\tilde{r}}\frac{\partial\beta}{\partial\tilde{r}}\right) + (M_2^2 - \tilde{a}^2)\left(\frac{1}{\tilde{r}^2}\frac{\partial^2\beta}{\partial\theta^2} + 2\frac{1}{\tilde{r}^2}\frac{\partial\alpha}{\partial\theta}\frac{\partial\beta}{\partial\theta}\right) + (\vec{M} \cdot \nabla M_1)\frac{\partial\beta}{\partial\tilde{r}} + (\vec{M} \cdot \nabla M_2)\frac{1}{\tilde{r}}\frac{\partial\beta}{\partial\theta} + \frac{M_1M_2}{\tilde{r}}\left[2\left(\frac{\partial^2\beta}{\partial\tilde{r}\partial\theta} + \frac{\partial\alpha}{\partial\theta}\frac{\partial\beta}{\partial\tilde{r}}\right) + \left(2\frac{\partial\alpha}{\partial\tilde{r}} - \frac{1}{\tilde{r}}\right)\frac{\partial\beta}{\partial\theta}\right]$$

and $\alpha = \ln(\tilde{\sigma}/\tilde{r}\chi_o)$, $\beta = k\tilde{r}$, $M_1 = U/a_\infty$, $M_2 = V/a_\infty$, $\lambda_o = \omega d_o/a_\infty$, χ_o a constant, $\vec{M} = (M_1, M_2, 0)$, $\tilde{a} = a_o/a_\infty$ and the expressions C, D, H_1 and H_2 are given in Ref. 10.

Coordinate Transformation

In view of the lack of an analytical solution of Eq. (15), an approximate solution to the corresponding finite-difference equation is sought. The domain in which Eq. (15) is to be solved is the half plane bounded by two concentric half circles with origin at the source, one of very small and one of very large radius, and the jet axis. Since the largest variations in α and β are expected for small $\tilde{r}$ and for small θ, the finite-difference grid needs to be dense in this region. For this purpose transformed variables are chosen[7] $\xi = \ln\tilde{r}$ and $\eta = \tan^{-1}(\zeta^{-2}\tan\theta)$ where $\zeta^2 < 1$. By proper choice on grid spacing ξ, η will result in a design grid spacing in $\tilde{r}$, θ as shown in Fig. 1. Then Eq. (15) in the new coordinates can be written as

$$\bar{f}(\xi,\eta;\alpha_\xi,\alpha_\eta,\alpha_{\xi\xi},\alpha_{\eta\eta},\beta,\beta_\xi,\beta_\eta,\beta_{\xi\xi},\beta_{\eta\eta}) = 0 \tag{16}$$

where $\bar{f}$ stands for F and G in Eq. (15).

The problem in the $\tilde{r}$, θ coordinates is thus transformed to a solution of a system of equations in a rectangular domain with coordinates ξ, η. The inner and the outer boundaries are mapped onto the lines $\xi = \xi_{\min}$ and $\xi = \xi_{\max}$, respectively. The plane $\eta = 0$ is the mapping of the downstream axis of symmetry of the jet; $\eta = \pi$ is the mapping of the upstream axis of symmetry of the jet in the source-jet configuration, Fig. 1.

Numerical Solution

Finite-Difference Equation

The scheme for solving Eq. (16) will be to replace the derivatives by central difference quotients, thus converting the equation to a difference equation. At the nodes of a grid work that subdivide the region of interest at which the function values are unknown, the difference equations are evaluated.

The region of interest in the ξ, η plane is divided by m and n lines parallel to the η and ξ axis, respectively. The distances between the lines are of equal width since the desired spacing of the radial lines in the physical $\tilde{r}$, θ plane can be adjusted through the selection ζ of the coordinate transformation $\eta = \eta(\theta)$.

Consider finite-difference approximations to the nonlinear elliptic Eqs. (16) in a closed domain and use a five-point molecule, at each interior point of the region, one obtains

$$f\left\{\xi_i, \eta_i, \frac{\alpha_{i+1,j} - \alpha_{i-1,j}}{2(\Delta\xi)}, \frac{\alpha_{i,j+1} - \alpha_{i,j-1}}{2(\Delta\eta)}, \frac{\alpha_{i+1,j} - 2\alpha_{i,j} + \alpha_{i-1,j}}{(\Delta\xi)^2}, \frac{\alpha_{i,j+1} - 2\alpha_{i,j} + \alpha_{i,j-1}}{(\Delta\eta)^2}, \beta_{i,j}, \frac{\beta_{i+1,j} - \beta_{i-1,j}}{2(\Delta\xi)}, \frac{\beta_{i,j+1} - \beta_{i,j-1}}{2(\Delta\eta)}, \frac{\beta_{i+1,j} - 2\beta_{i,j} + \beta_{i-1,j}}{(\Delta\xi)^2}, \frac{\beta_{i,j+1} - 2\beta_{i,j} + \beta_{i,j-1}}{(\Delta\eta)^2}\right\} = 0 \tag{17}$$

Equation (17) must be satisfied at every point (i,j) of a square net with interval size $\Delta\xi$ and $\Delta\eta$. These are systems of $2(m-2)(n-2)$ nonlinear algebraic equations

$$f_p(x) = 0 \qquad p = 1, 2, \ldots, q \tag{18}$$

where x is the unknown vector and $q = 2(m-2)(n-2)$.

Symmetry and Boundary Conditions

The jet axis is a line of symmetry. In the transformed ξ, η plane both the $j = 1$ and $j = n$ lines correspond to symmetry lines. The discrete symmetry conditions are represented by Markoff's formulas[11]

$$\begin{pmatrix}\alpha_{i,1}\\ \beta_{i,1}\end{pmatrix} = \frac{4}{3}\begin{pmatrix}\alpha_{i,2}\\ \beta_{i,2}\end{pmatrix} - \frac{1}{3}\begin{pmatrix}\alpha_{i,3}\\ \beta_{i,3}\end{pmatrix},$$

$$\begin{pmatrix}\alpha_{i,n}\\ \beta_{i,n}\end{pmatrix} = \frac{4}{3}\begin{pmatrix}\alpha_{i,n-1}\\ \beta_{i,n-1}\end{pmatrix} - \frac{1}{3}\begin{pmatrix}\alpha_{i,n-2}\\ \beta_{i,n-2}\end{pmatrix} \qquad (19)$$

$i = 2, 3, \ldots, m$. The approximation has $o(\Delta\eta^2)$ error, provided that α and β are sufficiently smooth.

The inner boundary condition is critical in the sense that it effectively specifies the characteristics of the source. Moretti and Slutsky's analysis[12] has verified that the uniform-flow part of the solution, which corresponds to a point source in a non-spreading jet, predominates close to the source. Hence, the appropriate inner boundary conditions are

$$\alpha = \tfrac{1}{2}\ln(1 - M_j^2 \sin^2\theta)^2 \left\{ \left[\frac{\tilde{a}}{\lambda_o \tilde{r}_\varepsilon} \frac{M_j \cos\theta}{(1 - M_j^2 \sin^2\theta)^{1/2}} \right]^2 + \left[\frac{(M_j^2 \sin^2\theta)^{1/2} - M_j \cos\theta}{1 - M_j^2} \right]^2 \right\},$$

$$\beta = \frac{\lambda_o \tilde{r}_\varepsilon}{\tilde{a}} \left[\frac{(1 - M_j^2 \sin^2\theta)^{1/2} - M_j \cos\theta}{1 - M_j^2} \right] - \tan^{-1}\left[\frac{\tilde{a}}{\lambda_o \tilde{r}_\varepsilon} \frac{M_j \cos\theta}{(1 - M_j^2 \sin^2\theta)^{1/2}} \frac{1 - M_j^2}{(1 - M_j^2 \sin^2\theta)^{1/2} - M_j \cos\theta} \right] \qquad (20)$$

where M_j is the exit Mach number and $\tilde{r}_\varepsilon$ is the small non-dimensional radius of the boundary. Numerical experimentation[7] shows that $\tilde{r}_\varepsilon = 0.25$ is generally adequate. The discrete outer boundary conditions which apply at a large non-dimensional radius $\tilde{r} = 100$ can be written as[7]

$$\begin{pmatrix}\alpha_{m,j}\\ \beta_{m,j}\end{pmatrix} = \frac{4}{2 + \Delta\xi}\begin{pmatrix}\alpha_{m-1,j}\\ \beta_{m-1,j}\end{pmatrix} - \frac{2 - \Delta\xi}{2 + \Delta\xi}\begin{pmatrix}\alpha_{m-2,j}\\ \beta_{m-2,j}\end{pmatrix}$$

$$j = 2, 3, \ldots, n-1 \qquad (21)$$

and contains an error of $o(\Delta\xi^2)$.

Iterative Method for Nonlinear Equations

The solution of systems of nonlinear simultaneous equation [Eq. (18)] subject to symmetry and boundary conditions Eqs. (19–21) is the final step in the solution of the problem. Recently, Ortega et al.[13] presented a comprehensive survey of the basic theoretical results about nonlinear equations in several variables as well as an analysis of the major iterative methods for their numerical solutions. Block iteration is chosen in the present application with each block consisting of the equations corresponding to l adjacent radial lines. These may be written in the vector form

$$fX = 0 \qquad (22)$$

where X is the $2(m-2)l$ dimensional column vector of unknowns and f the $2(m-2)l$ dimensional column vector of functions f_i; that is, $fX = [f_1(X), \ldots, f_{2(m-2)l}(X)]^T$,

$$X = (\alpha_{2,j}, \alpha_{3,j}, \ldots, \alpha_{m-1,j}; \ldots; \alpha_{2,j+l-1}, \alpha_{3,j+l-1}, \ldots, \alpha_{m-1,j+l-1}$$
$$\beta_{2,j}, \beta_{3,j}, \ldots, \beta_{m-1,j}; \ldots; \beta_{2,j+l-1}, \beta_{3,j+l-1}, \ldots, \beta_{m-1,j+l-1})^T$$

and

$$f = (F_{2,j}, F_{3,j}, \ldots, F_{m-1,j}; \ldots; F_{2,j+l-1}, F_{3,j+l-1}, \ldots, F_{m-1,j+l-1}$$
$$G_{2,j} G_{3,j}, \ldots, G_{m-1,j}; \ldots; G_{2,j+l-1}, G_{3,j+l-1}, \ldots, G_{m-1,j+l-1})^T$$

where T stands for the transpose of a matrix.

By the modified Newton's technique, if X^k is the kth approximation to the solution of Eq. (22), then

$$X^{k+1} = X^k - \omega^k f'(X^k)^{-1} fX^k, \qquad k = 0, 1, \ldots \qquad (23)$$

where the Jacobian matrix $f'(x^k) \equiv [\partial_i f_j(X^k)]$, i and $j = 1, 2, \ldots, N$ with $N = 2(m-2)l$ and where $\partial_i f_j(X^k)$ has been used to denote the partial derivative of f_j with respect to the ith variable and evaluated at X^k, and fX^k is the residual vector at the same point. The factors ω^k are chosen to insure that the iterative method be norm-reducing in the sense that

$$\|fX^{k+1}\| \leqq \|fX^k\|, \qquad k = 0, 1, \ldots \qquad (24)$$

holds in some norm.

In practice, one does not, of course, invert $f'(X^k)$ to carry out Eq. (23) but, rather, solves the linear system

$$f'(X^k)Y = -fX^k \qquad (25)$$

and adds the "correction" $\omega^k Y$ to X^k.

The steps in the procedure can be summarized as follows:

1) Assume an initial set of values $X^o = X^o(\alpha_{i,j}{}^o, \beta_{i,j}{}^o)$, $i = 2, 3, \ldots, m-1$, $j = 1, \ldots, n$, based upon experience, approximate solutions, or previously computed cases with conditions close to those desired.

2) Select block size l consistent with stability and storage requirements.

3) Start with $j = 2$.

4) Obtain an approximation to the Jacobian matrix numerically. That is, $\partial_i f_j(X)$ is computed by evaluating f_j for two different values of X_i and $(1+\delta)X_i$ where δ is a small perturbed number (for example, 10^{-6}). For simplicity, $f'(X^k)$ was kept constant as $f'(X^o)$.

5) Compute fX^k.

6) Solve the first-order linear system Eq. (25), by means of the method as outlined in Appendix B of Ref. 10, to obtain the increment Y.

7) Select a value ω^k such that Eq. (24) holds. This is done iteratively.[14] In the course of this calculation Eq. (23) and fX^{k+1} will have been computed.

8) Compute Eq. (21). If $j = 2$, 3, $n-l-1$, and $n-l$ the Eq. (19) will also be computed.

9) Test fX^{k+1} for convergence. If the iteration has not yet converged, repeat steps (6–8). Otherwise,

10) Increase j by 1 and repeat from step (4) until $j = n - l$.

Results and Discussion

The numerical example was computed for a jet described in Fig. 2 which has an exit Mach number $M_j = 0.62$, and for $\omega d_o/a_\infty = 1.145$, with a point source located at $2d_o$ downstream of the jet exit on the jet centerline, $\theta = 0°$. Comparison of the results of this work, Fig. 3, is limited to only two references, one numerical,[7] and the other experimental.[15] One should note that Schubert's result had a Mach number $M_j = 0.7$, $\omega d_o/a_\infty = 1.055$ and Grande's experiments had Mach numbers $M_j = 0.5$ and 0.9, $\omega d_o/a_\infty = 1.055$. In this figure all results are obtained for a point source located at $2d_o$ downstream of the nozzle on the jet centerline. The present theory shows qualitative agreement with experiment, and this agreement seems to be better than the corresponding comparison with the numerical results of

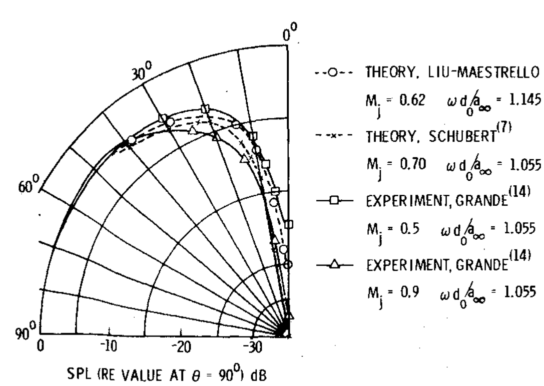

Fig. 3 Polar directivity at distance $100d_o$ from source.

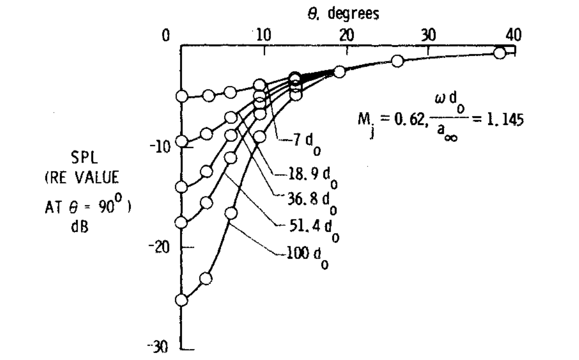

Fig. 4 Noise directivity at various distances from the source.

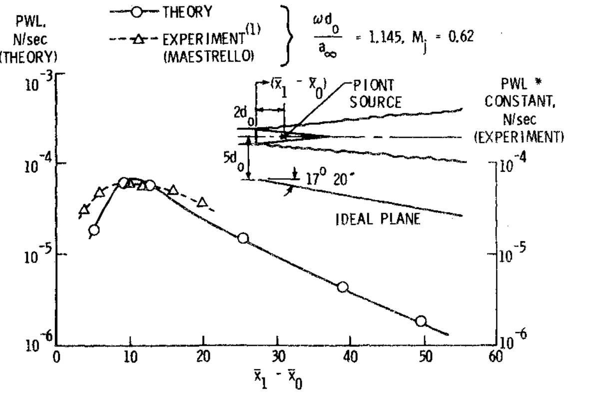

Fig. 6 Variation of acoustic power along the plane.

Ref. 7. One possible reason could be attributed to the fuller description of the mean flowfield of the jet; however, in order to better reassess the error involved in the prediction scheme an experiment would have to be conducted using an experimental point source in the present jet. In addition, it is believed that the directivity at small angles from the jet axis would be better approximated if the scattering due to turbulence were included. This improvement could account for an additional 3–5 db change in the directivity pattern in Fig. 3.

Figure 4 shows the directivity pattern at various distances from the source. The deep valley along the jet exit due to the refraction effect increases with the distances from the source, a behavior similar to the one indicated by Schubert.[7]

This analysis has been further used to evaluate the acoustic energy density flux through an ideal plane[1] at $5d_o$ away from the jet exit and inclined at an angle of 17°20′. The plane is in the region where the homogeneous wave equation is reasonably well satisfied. Knowledge of the acoustic energy density flux, pv_n, along the plane provides the information on the relationship between its distribution and the source location. This relationship is the first step toward establishing the real source location and strength from the knowledge of the acoustic flux on the plane.[1] The distribution of the acoustic power per unit area is shown in Fig. 5. This distribution indicates that the peak value occurs at approximately $10d_o$ downstream of the exit plane. In effect, the distribution of the acoustic flux drifts downstream from $2d_o$ to $10d_o$ due to the mean flow.

Figure 6 shows the computed distribution of the acoustic power per unit length along the plane for a point source along with experimental distribution obtained from real sources. The behavior of these two distributions is quite similar for $\omega d_o/a_\infty = 1.145$, $M_j = 0.62$ once the amplitude of the real jet is multiplied by a normalized constant.

Computation results can be improved by including 3 effects which have been neglected in the present analysis. The first is the effect of turbulence scattering which has been mentioned previously. The second is by using distribution of sources, either monopoles or quadrupoles, embedded around and along the shear layer and drifting with the local mean flow. The third involves the re-examination of the present analysis in which the source in the jet has been described as a harmonic source rather than nonperiodic source. The latter requires the solution of a hyperbolic system of equations instead of an elliptic one. All these possibilities are being investigated at the present time in order to further improve the description of sound propagation through a real jet flowfield.

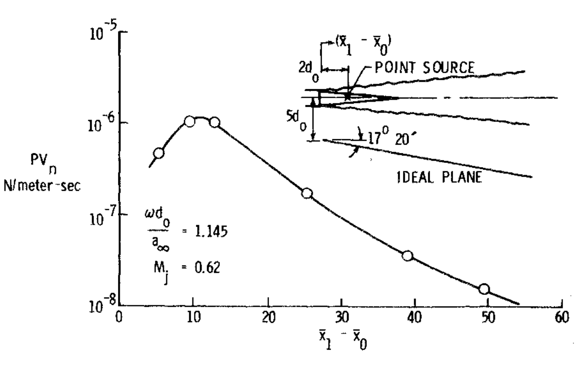

Fig. 5 Acoustic power unit area along the plane.

References

[1] Maestrello, L., "On the Relationship Between Acoustic Energy Density Flux Near the Jet and Far Field Acoustic Intensity," TN D-7269, Oct. 1973, NASA.

[2] Doak, P. E., "An Introduction to Sound Radiation and Its Sources," Rept. 154, Oct. 1967, Institute of Sound and Vibration Research, University of Southampton, England.

[3] Lilley, G. M., "The Generation of Sound in a Mixing Region," Vol. IV, Chap. 2, TR-72-53, July 1972, Air Force Aero Propulsion Lab., Wright-Patterson Air Force Base, Ohio.

[4] Mungur, P., Plumblee, H. E., and Doak, P. E., "On the Influence of Jet Flow on Sound Radiation," presented at the 111ème Colloque d'Acoustique Aeronautique, Toulouse, France, March 1972.

[5] Plumblee, H. E., "Noise Radiated From Sources Upstream of the Nozzle Exit Plane," Vol. IV, Chap. 3, TR-72-53, July 1972, Air Force Aero Propulsion Lab., Wright-Patterson Air Force Base, Ohio.

[6] Graham, E. W. and Graham, B. B., "Theoretical Study of the Effect of Refraction on Noise Produced by Turbulence in Jets," CR-2390, March 1974, NASA.

[7] Schubert, L. K., "Numerical Study of Sound Refraction by a Jet Flow II, Wave Acoustic," *Journal of the Acoustical Society of America*, Vol. 51, No. 2, Pt. 1, 1972, pp. 447–463.

[8] Mani, R., "A Moving Source Problem Relevant to Jet Noise," *Journal of Sound and Vibration*, Vol. 25, No. 2, Nov. 1972, pp. 337–347.

[9] Pao, S. P., "Aerodynamic Noise Emission from Turbulent Shear Layers," *Journal of Fluid Mechanics*, Pt. 3, Vol. 59, July 1973, pp. 451–479.

[10] Liu, C. H. and Maestrello, L., "Propagation of Sound Through a Real Jet Flow Field," AIAA Paper 74-5, Washington, D.C., 1974.

[11] Abramowitz, M. and Stegun, I. A., *Handbook of Mathematical Functions*, Dover, New York, 1965.

[12] Moretti, G. and Slutsky, S., "The Noise Field of a Subsonic Jet," TR 150 (AFOSR TN-59-1310), 1959, General Applied Science Lab., Inc., New York.

[13] Ortega, J. M. and Rheinboldt, W. C., *Iterative Solution of Nonlinear Equations in Several Variables*, Academic Press, New York, 1970.

[14] Broden, C. G., "A Class of Methods for Solving Nonlinear Simultaneous Equations," *Mathematics of Computations*, Vol. 19, 1965, pp. 577–593.

[15] Grande, E., "Refraction of Sound by Jet Flow and Jet Temperature II," UTIAS, TN 110, Dec. 1966, or CR 840, 1967, NASA.